LVI SBPO SIMPÓSIO BRASILEIRO DE PESQUISA OPERACIONAL
DE 04 ATÉ 07 NOVEMBRO 2024
FORTALEZA | CEARÁ

Main bearing degradation prediction in wind turbines via quantum support vector machine regression

Samuel Bezerra da Gama Neto[1]
samuel.gneto@ufpe.br

Gustavo de Novaes Pires Leite[2]
gustavonovaes@recife.ifpe.edu.br

Januário Leal de Moraes Vieira[2]
januarioleal@recife.ifpe.edu.br

Alvaro Antonio Ochoa Villa[1,2]
ochoaalvaro@recife.ifpe.edu.br

Enrique Lopez Droguett[3]
eald@ucla.edu

Alexandre Carlos Araújo da Costa[1,4]
alexandre.acosta@ufpe.br

Marrison Gabriel Guedes de Souza[5]
marrison.souza@neog.com.br

[1]Federal University of Pernambuco, Cidade Universitaria, s/n, Recife, PE, CEP 50740-550, Brazil
[2]Federal Institute of Education, Science and Technology of Pernambuco, Campus Recife, DACI/CACTR, Brazil
[3]Center for Reliabilty Science and Engineering, Garrick Institute for the Risk Sciences, University of California, Los Angeles, CA 90095, USA
[4]Center for Renewable Energy of the Federal University of Pernambuco, Brazil
[5]NEOG – New Energy Options Geração de Energia, Brazil

ABSTRACT

To mitigate energy production losses in wind energy sector, maintenance activities should be scheduled during periods of low wind. An alternative to help achieve this goal is by predicting the remaining useful life (RUL) of components, which indicates the estimated time a component can function before experiencing critical failure. In this work, a framework is applied to predict the main bearing degradation using real operational data, collect by the SCADA system, of three wind turbines. Quantum support vector machine (QSVM), a field that merges principles from quantum mechanics with the classical SVM model, is explored with six distinct feature maps. The methodology employs a strategy to overcome data scarcity, by partitioning data into training, validation, and test subsets. The results demonstrated that the angular QSVM overcame the classical SVM model, with R2 score of 0.8532 and RMSE of 0.0796, which highlights the potential of quantum computing to achieve accurate predictions.

KEYWORDS. Wind turbine. Remaining useful life. Quantum support vector machine.

Paper topics (SE-QPO - Quantum Methods and their Applications in Operational Research, EN&PG - OR in the Energy, Oil and Gas Area)

DOI: 10.59254/sbpo-2024-193539
https://proceedings.science/p/193539?lang=pt-br

1. Introduction

Driven by population growth, economic development, and environmental concerns over greenhouse gas emissions, wind energy is emerging as one of the most competitive and least harmful renewable energy technologies [Summerfield-Ryan and Park 2023].

In rotating machinery, bearings are crucial components that support loads and minimize friction. In wind turbines (WTs), bearings are found in the pitch system, main shaft, gearbox, yaw system, and generator. According to [Azevedo et al. 2016], bearing failures are a common cause to influence for WT component breakdowns, highlighting the critical importance of bearing condition monitoring.

Another important issue is that WTs are devices that convert the kinetic energy of the wind into rotational motion, which is transferred from the blades to the generator for the production of electrical energy. To optimize energy production in wind farms, maintenance activities should be prioritized during periods of low wind [Papadopoulos, Coit and Ezzat 2021].

In this context, machine learning (ML) algorithms have been applied for fault detection, diagnosis, and prognosis in WTs. [Leite et al. 2023] employed ML models for anomaly detection of the generator non-drive end bearing using vibration data. To the same wind farm, [Munguba et al. 2024] used ensemble techniques for ML models to fault detection in WT drivetrain components. From a prognostic perspective, [Yan et al. 2020] proposed support vector machine (SVM) and hybrid degradation tracking model to predict the remaining useful life (RUL) of bearings.

Quantum machine learning (QML) is an emerging field of research that intersects ML and quantum computing. QML uses the principles of quantum mechanics to enhance ML algorithms and achieve quantum advantage, enabling the solution of complex problems for classical ML models [Melnikov et al. 2023]. According to [Cerezo et al. 2022], QML can offer advantages in many applications, such as quantum simulation, quantum machine perception, data analysis, and enhanced quantum computing.

In this case, this study presents an application of QML to bearing condition monitoring, which could serve as a supplementary tool for wind farm maintenance teams. Thus, the main objectives of this research are: (1) degradation prediction of WT main bearing using real operational data from the supervisory control and data acquisition (SCADA) system of a wind farm located in Brazil, (2) to apply QML models for a regression task, and (3) to compare the performance of the QML approach over a classical ML model.

This paper is organized as follows. Section 2 explains the theoretical foundation. Section 3 presents the framework for the RUL profile definition and the QML setup. Section 3 provides the results and discussion. Section 4 presents the conclusions and future research directions.

2. Quantum support vector machine (QSVM)

Quantum support vector machine (QSVM) is a variation of SVM that utilize the principles of quantum mechanics to estimate the kernel function $k(\vec{x}_i, \vec{x}_j)$ using quantum circuits. In QML, the most basic unit of information is the qubit $|\psi\rangle$ that can exist simultaneously in multiple states between the basis vector, $|0\rangle = [1\ 0]^T$ and $|1\rangle = [0\ 1]^T$. The potential of QML over classical computing are due the quantum phenomena that a qubit can exhibit [Garg and Ramakrishnan 2020]:

- Superposition: A qubit can exist in a combination of the two states, $|0\rangle$ and $|1\rangle$, by $|\psi\rangle = \alpha|0\rangle + \beta|1\rangle$. Where α and β are complex amplitudes that describes the probabilities $|\alpha|^2$ and $|\beta|^2$ of $|\psi\rangle$ be in the state $|0\rangle$ or $|1\rangle$, respectively;
- Entanglement: Defines a correlation between composite quantum system. If $|\psi\rangle$ can be described as $|\psi\rangle = |\psi_1\rangle \otimes |\psi_2\rangle \otimes \cdots \otimes |\psi_n\rangle$, is said to be in a separable state. Otherwise it is entangled.

DOI: 10.59254/sbpo-2024-193539
https://proceedings.science/p/193539?lang=pt-br

In quantum computing, these phenomena are achieved by the use of quantum gates, which are represented by unitary matrices U, on quantum circuits. A qubit is manipulated in a sequence of gates, as described by $|\psi_{i+1}\rangle = U|\psi_i\rangle$ with $U^\dagger U = UU^\dagger = I$. These operations can be classified as: single-qubit or multi-qubit gates, and parametric or non-parametric gates [Schuld and Petruccione 2018]. The most single-qubit gates known are the Hadamard gate H and the Pauli matrices X, Y and Z, which represents 180º rotation around the axis x, y and z, as defined in Equation (1). In the case of multi-qubit gates, an example is the C-NOT gate that is applied for two qubits, the first qubit being considered the control qubit and the second qubit the target, according to Equation (2).

$$H = \frac{1}{\sqrt{2}}\begin{bmatrix}1 & 1\\ 1 & -1\end{bmatrix};\ X = \begin{bmatrix}0 & 1\\ 1 & 0\end{bmatrix};\ Y = \begin{bmatrix}0 & -i\\ i & 0\end{bmatrix};\ Z = \begin{bmatrix}1 & 0\\ 0 & -1\end{bmatrix} \quad (1)$$

$$CNOT = \begin{bmatrix}1 & 0 & 0 & 0\\ 0 & 1 & 0 & 0\\ 0 & 0 & 0 & 1\\ 0 & 0 & 1 & 0\end{bmatrix} \quad (2)$$

In classical SVM, the regression function $f(x)$ is obtained with ε deviation from the actual values y_i, described by a minimization problem to find the optimal hyperplane, as defined in Equation (3) [Smola and Schölkopf 2004]. Thus, SVM performance relies in identifying the best kernel function.

$$f(x) = \sum_{i=1}^{n}(\alpha_i - \alpha_i^*) \cdot k(\vec{x}_i, \vec{x}) + b \quad (3)$$

where α_i and α_i^* are Lagrange multipliers, $k(\vec{x}_i, \vec{x})$ is the kernel function that allows for the computation of similarity between pairs of data, and the parameter b can be obtained using the Karush–Kuhn–Tucker (KKT) conditions.

Relating to QSVM, the quantum kernel estimation (QKE) used in SVM models is obtained through a feature map. A feature map ϕ is a technique to transform a classical information into a quantum state. Thus, the QKE is described in Equation (4) and the quantum circuit used is illustrated in Figure 1, as defined in [Liu, Arunachalam and Temme 2021].

$$k(\vec{x}_i, \vec{x}_j) = \left|\langle\phi(\vec{x}_j)|\phi(\vec{x}_i)\rangle\right|^2 = \left|\langle 0^{\otimes n}|U(\vec{x}_j)^\dagger U(\vec{x}_i)|0^{\otimes n}\rangle\right|^2;\ |\phi(\vec{x})\rangle = U(\vec{x})|0\rangle^{\otimes n} \quad (4)$$

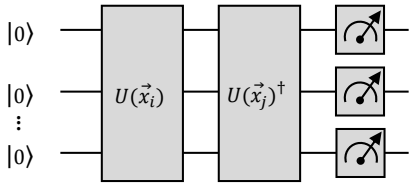


Figure 1. Quantum kernel estimation circuit.

3. Methodology

Extending the work of [Vieira et al. 2024], this study is intended to the prediction of WTs main bearing degradation using operational data from a wind farm located in northeastern Brazil. Three 1MW WTs of the same design, each with recorded main bearing failures were selected. Table 1 shows the corrective maintenance interventions dates of each WT.

In this work, the approach applied data from the SCADA system, which collects real-time operational information and provides maximum, minimum, average, and standard deviation values at 10-minute intervals for each analyzed variable [Astolfi et al. 2021]. It was considered the following variables: average main bearing temperature, average ambient temperature, average wind speed, maximum and minimum generator speed, and average active power.

DOI: 10.59254/sbpo-2024-193539
https://proceedings.science/p/193539?lang=pt-br

Table 1. Maintenance interventions dates.

Turbine	Stop date	Start date	Downtime (days)
WT01	2018-06-11	2018-07-22	41
WT02	2018-07-27	2018-09-09	44
WT03	2018-09-28	2018-12-01	64

Figure 2 shows the steps implemented for the methodology proposed, wherein the main steps are: (1) preprocessing, which consists of operational, outlier removal, resampling and seasonal decomposition, (2) quantum model, involves the use of quantum circuits to map the input data to a high-dimensional feature space to be used in a classical SVM model, and (3) performance evaluation, determines how accurately the model fits the data to make predictions.

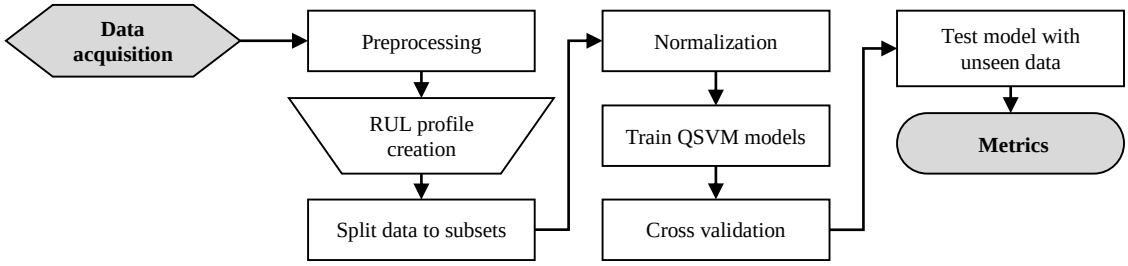


Figure 2. Flowchart of QSVM method.

The procedure considered the main bearing temperature, as an increase in bearing temperature is a possible indicative of a problem due friction, inadequate lubrication, or abnormal wear. According to [Pandit et al. 2023], main bearing temperature is frequently observed. This is related to its significant size and low rotational speed, which allow for easy detection of any anomalies in its behavior.

The first step of the methodology is preprocessing, a stage that involves preparing and cleaning the data to ensure that it is within operational limits and correspond to operation periods of the WTs. The steps involved in this stage were:

1. Operational conditional filtering: To remove periods of machine stop, wind speed above cut-in, and remove temperature above operational limits. These filters are listed in Table 2;
2. Creation of a new variable: To remove the influence of the ambient temperature on main bearing temperature due to heat transfer mechanisms, as defined by [Wiese et al. 2020 and Mello et al. 2021]. The new corrected temperature is defined as $T_{corrected} = T_{main\ bearing} - T_{ambient}$;
3. Outlier removal: To eliminate values above 98% of the percentile of the time series and bellow 10 ºC of the main bearing corrected temperature;
4. Resampling data for one-day timestamp;
5. Not a number removal;
6. Seasonal decomposition: To mitigate the impact of the trend within the time series, employing an additive model over a 7-day period.

Table 2. Operational conditional filtering.

Filter	Description	Limits
1	To remove periods of WT stop	maximum generator speed > 1200 minimum generator speed >= 1198
2	Captures the instances when the WT is producing active power	average wind speed >= 3.5
3	Above operational limits	average ambient temperature <= 50

DOI: 10.59254/sbpo-2024-193539
https://proceedings.science/p/193539?lang=pt-br

After applying operational conditional filtering, the average main bearing temperature times series is presented in Figure 3. It can be noticed that only WT01 reached the main bearing temperature alarm.

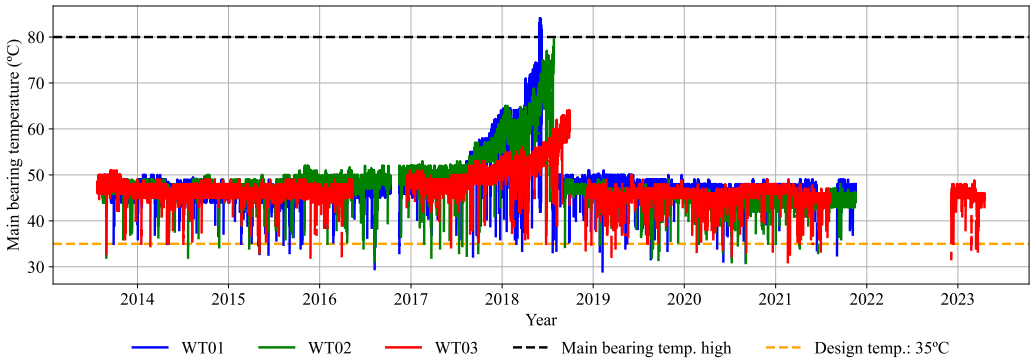


Figure 3. Filtered average main bearing temperature times series

To reduce processing time for the quantum models, another preprocessing step was implemented, distinct from the approach utilized by [Vieira et al. 2024]. This step involved resampling the time series to a monthly timestamp and not a number removal. The final dataset contains 84 samples with 13 features. Figure 4 presents the final average main bearing temperature times series.

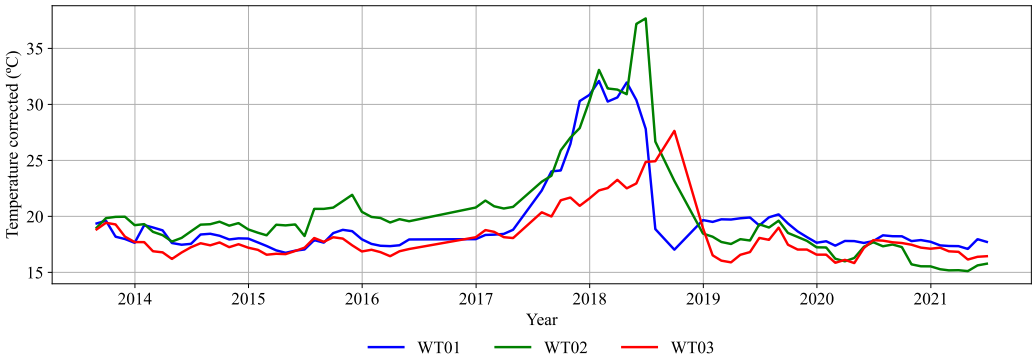


Figure 4. Final average main bearing temperature times series.

The second critical step of the methodology is to establish the RUL profile. This process involved the definition of the first time prediction time (FPT), failure threshold time (FTT) and restoration instant (RT), which are defined bellow as:

- FPT: Corresponds to the start of the degradation;
- FTT: Indicates the moment of complete component failure;
- RT: Represents the instant that the component is in fully functional state after repair or replacement.

RUL is defined as the time interval between FPT and FTT. After preprocessing, the time series of temperature corrected were analyzed graphically to determine the values of FPT, FTT and RT, as presented in Table 3.

As described by [Vieira et al. 2024], the RUL profile for monthly timestamp was defined in four intervals, where '1' represents a healthy state and '0' represents a degraded state. This classification process is explained as follows:

DOI: 10.59254/sbpo-2024-193539
https://proceedings.science/p/193539?lang=pt-br

- Interval 1: Period before FPT, classified as healthy state;
- Interval 2: Corresponds to the period of temperature increase up to the maximum recorded temperature, with classification done by linear interpolation from the healthy state to the minimum data classification value, defined as $C_{min} = 1 - T_{normalized}$. The temperature ($T_{normalized}$) is obtained by the normalization of the WT maximum temperature across all WTs;
- Interval 3: Period corresponding to the maximum temperature range, classified as the 0 state;
- Interval 4: After the RT, classified as healthy state.

Table 3. Historical FPT, FTT and RT values established graphically.

Turbine	FPT	FTT	RT
WT01	2017-04	2018-05	2018-07
WT02	2016-06	2018-06	2018-09
WT03	2017-06	2018-09	2018-12

Figure 5 illustrates the defined RUL profile for a monthly timestamp of each WT analyzed. As observed in Table 3 and Figure 4, WT01 and WT03 exhibited a higher speed of degradation compared to WT02. This indicates varying degradation dynamics, which impact maintenance scheduling.

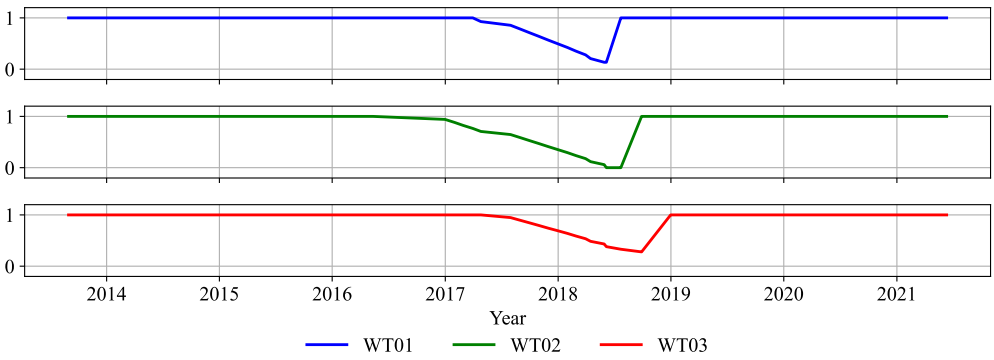


Figure 5. RUL profile.

Thus, the features used to predict the degradation indicator were: average temperature corrected, average wind speed and average active power. These features were employed in the QSVM model, which will be compared to the SVM.

In this analysis, a cross validation (CV) scheme was established to avoid overfitting and to determine the best hyperparameter combination, so the results of the quantum models can be compared to the outcomes of the classical SVM implemented by [Vieira et al. 2024], but this time with a monthly timestamp. The CV approach consist in split data to subsets of training, validation and test data, as presented in Table 4.

Table 4. Strategy for training, validation, and test subsets.

Simulation case	Training	Validation	Test
SC01	WT01	WT02	WT03
SC02	WT01	WT03	WT02
SC03	WT02	WT01	WT03
SC04	WT02	WT03	WT01
SC05	WT03	WT01	WT02
SC06	WT03	WT02	WT01

DOI: 10.59254/sbpo-2024-193539
https://proceedings.science/p/193539?lang=pt-br

3.1 QSVM approach

The QSVM approach involves applying the quantum kernel method. This method functions as a similarity measure analogous to the classical kernel trick used in SVM. These similarity measures are calculated by executing quantum circuits implemented using Python libraries as PennyLane and Qiskit, which simulate error-free quantum phenomena.

In this work, only feature maps previously proposed in the literature were considered, as they have demonstrated good results in applications such as in the medical field [Akpinar, Islam, and Oduncuoglu 2024], wind turbine fault detection [Correa-Jullian et al. 2022], and regression problems [Zhou et al. 2024]. A hardware with intel i7-7500U CPU and 8GB of RAM was used in this research.

The following feature maps, described by [Schuld 2021], implemented in Pennylane used were: (1) Amplitude: Employs n qubits to encode 2^n features into their amplitude vector, given $\|x\|^2 = \sum_i |x_i|^2 = 1$ to $\phi: x \rightarrow |x\rangle\langle x| = \sum_{i,j=1}^{N} x_i x_j^* |i\rangle\langle j|$, where x is a data point and N is the number of features, (2) Angular: Maps N features in the rotation angles of the Pauli matrices of n qubits.

For the QSVM models implemented in Qiskit, the feature maps are based on the work of [Havlíček et al. 2019]. The quantum circuit can be expressed as $\mathcal{U}_\Phi(x) = \prod_d U_{\Phi(x)} H^{\otimes n}$, where d denotes the circuit depth layer, H is the had Hadamard gate and $U_{\Phi(x)}$ is defined in Equation (5).

$$U_{\Phi(x)} = \exp(i \sum_{S \subseteq [n]} \Phi_s(x) \prod_{i \in S} P_i) \tag{5}$$

where $P_i \in \{I, X, Y, Z\}$ (Pauli matrices), S represents the associations between different qubits and $\Phi_s(x)$ is a nonlinear function defined in Equation (6).

$$\Phi_s(x) = \begin{cases} x_i \ if \ S = \{i\} \\ \prod_{j \in S} (\pi - x_j) \ if \ |S| > 1 \end{cases} \tag{6}$$

Table 5 shows the QSVM setup. Each feature map was evaluated for every simulation scenario outlined in Table 4. Initially, the model was trained using the training dataset, followed by evaluation with the validation set. The hyperparameters were determined through a grid search. Finally, the models were assessed using the test data.

Table 5. QSVM setup.

Parameters	Description/Value
Feature map	Amplitude, Angular, PauliFeatureMap-X, PauliFeatureMap-Y, ZFeatureMap and ZZFeatureMap
Normalization	MinMaxScaler
Regularization parameter	C = [0.1, 1.0, 10.0]
Metric for CV	R2 score

3.2 Performance evaluation

Three key metrics were used to evaluate the performance of the models:

1. Root mean square error (RMSE): Measures the difference between the predicted values $\tilde{y}$ and the actual values y, according to Equation (7). RMSE is sensitive to outliers, because it amplifies the effect of large errors. ideally, the RMSE value should be close to zero;
2. Mean absolute error (MAE): Similar to RMSE, but without penalization for outliers as expressed in Equation (8);

DOI: 10.59254/sbpo-2024-193539
https://proceedings.science/p/193539?lang=pt-br

3. R2 score: Evaluates the variability explained by the regression model, with a target value of 1, as defined in Equation (9).

$$RMSE\ (y, \tilde{y}) = \sqrt{\frac{1}{n}\sum_{i=1}^{n}(y_i - \tilde{y}_i)^2} \tag{7}$$

$$MAE\ (y, \tilde{y}) = \frac{1}{n}\sum_{i=1}^{n}|y_i - \tilde{y}_i| \tag{8}$$

$$R^2\ (y, \tilde{y}) = 1 - \frac{\sum_{i=1}^{n}(y_i - \tilde{y}_i)^2}{\sum_{i=1}^{n}(y_i - \overline{y}_i)^2} \tag{9}$$

4. Results and discussions

This section presents the results of six QSVM models applied to each simulation case, with data from the SCADA system of three wind turbines, to predict the degradation indicator of main bearing. Firstly, the residual error using RMSE and MAE are shown. Secondly, the performance of the quantum regression models is compared with R2 score. Then, the best QSVM model is compared to the classical SVM model. Finally, an evaluation of the average behavior exhibited by the analyzed models is conducted.

Figure 6 shows the RMSE and MAE metric values for the test dataset of all simulation cases. The RMSE and MAE results for all QSVM models were below 0.3 and 0.2, respectively. Across all case studies, the Angular and PauliFeatureMap-X models exhibited the lowest values, while the PauliFeatureMap-Y model produced the highest values. Additionally, the PauliFeatureMap-X model demonstrated low variability across all simulation cases for both RMSE and MAE metrics.

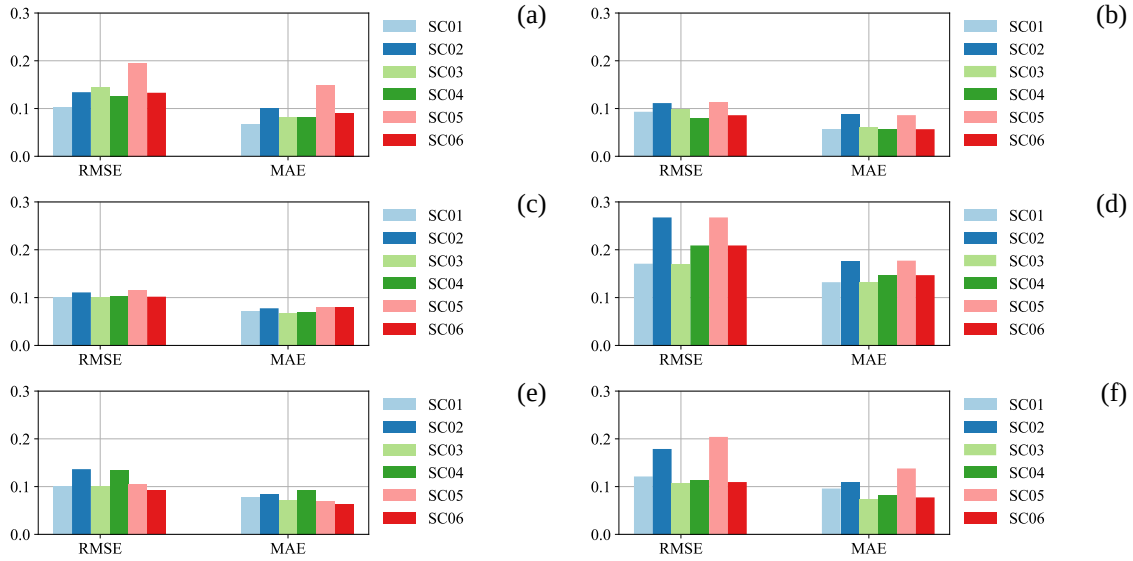


Figure 6. Results of RMSE and MAE for the QSVM models for the test set. (a) Amplitude; (b) Angular; (c) PauliFeatureMap-X; (d) PauliFeatureMap-Y; (e) ZFeatureMap; (f) ZZFeatureMap.

Table 6 summarizes the overall RMSE and MAE results. The Angular model achieving the highest performance by achieving RMSE and MAE values closer to zero. On the other hand, the PauliFeatureMap-Y model exhibited the lowest performance.

For the R2 score metric, Figure 7 presents the results for the test set. Among the models, only Angular, PauliFeatureMap-X, and ZFeatureMap achieved results above 0.75, demonstrating high capacity in capturing the variability. In contrast, the PauliFeatureMap-Y models exhibited negative values. The highest R2 score value was 0.8532 for the Angular model with the SC04 test

DOI: 10.59254/sbpo-2024-193539
https://proceedings.science/p/193539?lang=pt-br

data, while the lowest value was -0.0453 for the PauliFeatureMap-Y model in both SC01 and SC03 cases.

Table 6. Overall results of RMSE and MAE for the test set.

Metric	Maximum			Minimum		
	Model	SC	Value	Model	SC	Value
RMSE	PauliFeatureMap-Y	SC02, SC05	0.2676	Angular	SC04	0.0796
MAE	PauliFeatureMap-Y	SC02, SC05	0.1772	Angular	SC01	0.0563

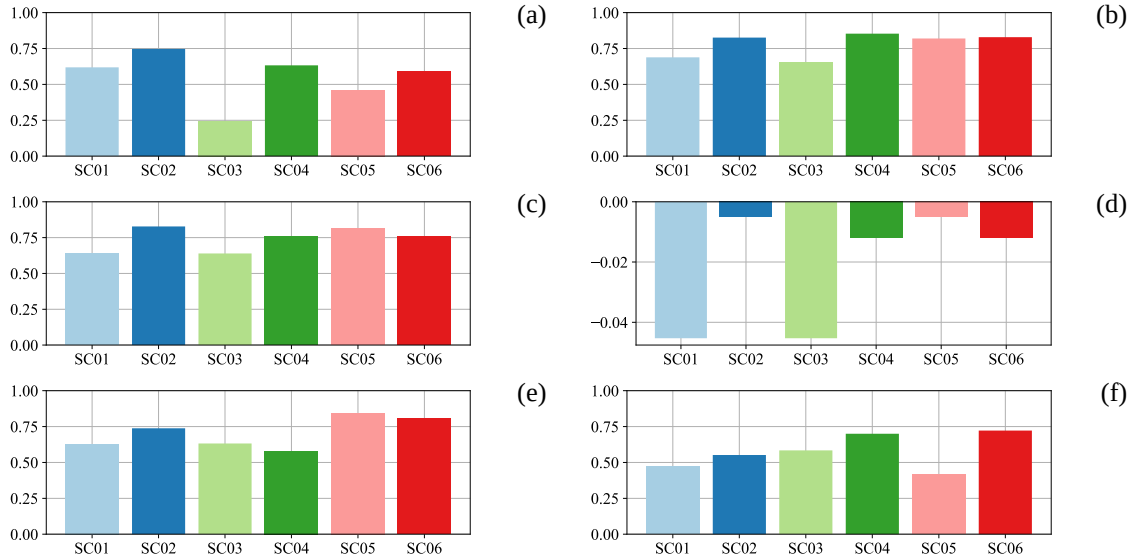


Figure 7. Results of R2 score for the QSVM models for the test set. (a) Amplitude; (b) Angular; (c) PauliFeatureMap-X; (d) PauliFeatureMap-Y; (e) ZFeatureMap; (f) ZZFeatureMap.

In order to evaluate the performance of the QSVM models for regression, the SVM model with a polynomial kernel function and parameters for grid search C = [0.1, 1.0, 10.0] and degree = [5, 6, 7, 8, 9] was employed, as proposed by [Vieira et al. 2024], using the same features as the QSVM models. In this analysis, the Angular model was chosen due to its superior performance relative to the other quantum models. Figure 8 shows the RMSE, MAE and R2 score metrics for the classical and quantum models.

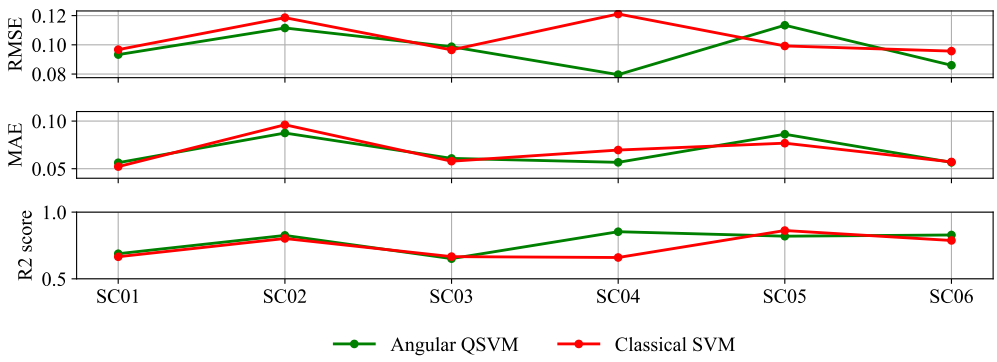


Figure 8. RMSE, MAE and R2 score for the Angular QSVM and Classical SVM models.

A comprehensive analysis of Figure 7 reveals that the quantum model outperformed the classical model, in four simulation cases, on all evaluated metrics. Figure 9 presents the RUL

DOI: 10.59254/sbpo-2024-193539
https://proceedings.science/p/193539?lang=pt-br

profile prediction for the test set of SC04 simulation case of the Angular, PauliFeatureMap-X and Classical model.

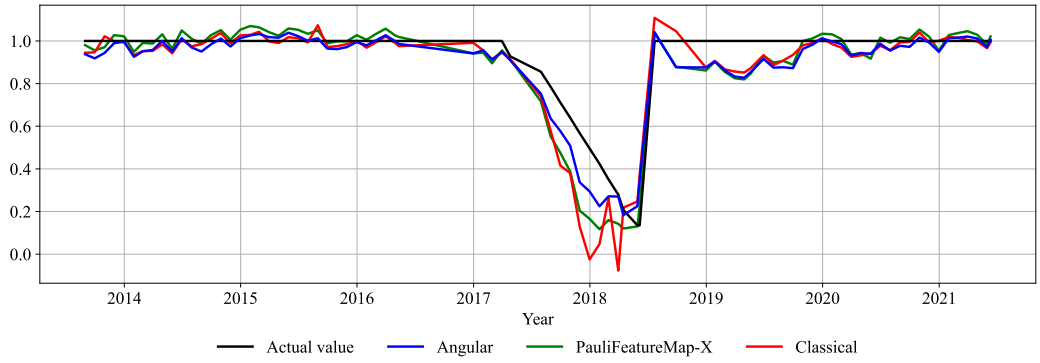


Figure 9. RUL profile prediction.

Table 7 summarizes the performance of the QSVM and SVM models on validation and test datasets by the mean value of RMSE, MAE and R2 score. In both stages, the PauliFeatureMap-Y model underperformed compared to the other models. In relation to the Classical model, the best QSVM model demonstrated superior performance on all metrics and stages. For the test set, the Angular model outperformed across all metrics. Figure 10 illustrates the mean values of RMSE, MAE, and R2 score for the test set, organized in ascending order.

Table 7. Mean values of RMSE, MAE and R2 score for the validation and test set.

Model	Validation			Test		
	RMSE	MAE	R2 score	RMSE	MAE	R2 score
Amplitude	0.1210	0.0748	0.6629	0.1396	0.0949	0.5489
Angular	0.0762	**0.0538**	0.8630	**0.0971**	**0.0674**	**0.7778**
PauliFeatureMap-X	0.0715	0.0563	0.8764	0.1053	0.0742	0.7388
PauliFeatureMap-Y	0.2158	0.1521	-0.0208	0.2158	0.1521	-0.0208
ZFeatureMap	**0.0659**	0.0542	**0.8937**	0.1119	0.0764	0.7047
ZZFeatureMap	0.0686	0.0597	0.8900	0.1392	0.0962	0.5746
Classical	0.0776	0.0548	0.8471	0.1046	0.0683	0.7408

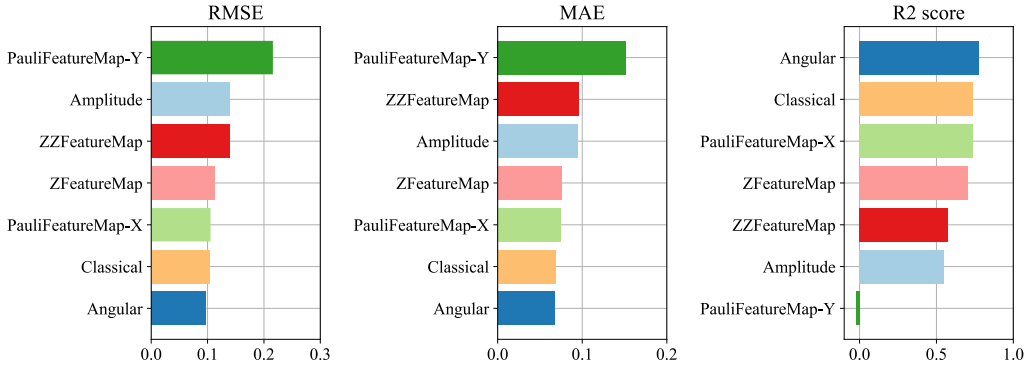


Figure 10. Mean values of RMSE, MAE, and R2 score for the test set.

The three top-performing quantum models in terms of lowest average RMSE, MAE, and highest average R2 score are: Angular, PauliFeatureMap-X, and ZFeatureMap. Among the quantum models, Angular outperformed the Classical model.

DOI: 10.59254/sbpo-2024-193539
https://proceedings.science/p/193539?lang=pt-br

5. Conclusions

In this study, QSVM models were employed to identify the degradation in wind turbine main bearing of a wind farm located in Brazil, using operational data from the SCADA system. Three wind turbines with main bearing failures were subjected to a procedure to obtain the RUL profile, which included operational filters, corrected temperature definition, outlier removal and resampling. Furthermore, a cross validation was conducted to help with hyperparameter definition and overfitting mitigation.

The framework of QSVM is similar to classical SVM, the difference lies in the use of a quantum circuit to calculate the kernel function, which in this application used six feature maps: Amplitude, Angular, PauliFeatureMap-X, PauliFeatureMap-Y, ZFeatureMap and ZZFeatureMap.

The main findings of this research were: (1) Regarding the simulation cases, the Angular model for case SC04 achieved the best performance with an RMSE of 0.0796 and an R2 score of 0.8532 for the test set. In contrast, the PauliFeatureMap-Y exhibited unsatisfactory performance; (2) Incorporating entanglement gates using the ZZFeatureMap did not lead to any improvement in performance compared to the ZFeatureMap; (3) The overall mean results between the simulation cases demonstrated that the best-performing quantum models were Angular, PauliFeatureMap-X, and ZFeatureMap. However, the Angular model achieved superior metrics with RMSE, MAE, and R2 scores of 0.0971, 0.0674, and 0.7778, respectively; (4) In a direct comparison of quantum and classical models, the Angular model outperformed the classical model by almost 5% in R2 score, while also achieving lower RMSE and MAE values, closer to zero.

These findings demonstrate the potential of incorporating quantum mechanical principles into machine learning models in problems of engineering. It is important to note that the study was conducted in an error-free quantum simulation environment, and the effects of quantum hardware noise were not considered. Further research should focus in the application of parametrized quantum circuits to predict the degradation state of bearings, to improve the accuracy of the quantum approach.

6. Acknowledgements

This study was financed in part by the Coordenação de Aperfeiçoamento de Pessoal de Nível Superior - Brasil (CAPES) - Finance Code 001. The information in this study was obtained during the development of a Research and Development - R&D project supported by Rio Amazonas SA and approved by the Brazilian Regulatory Agency ANEEL

References

Akpinar, E., Islam, S., and Oduncuoglu, M. (2024). Evaluating the Impact of Different Quantum Kernels on the Classification Performance of Support Vector Machine Algorithm: A Medical Dataset Application. *arXiv preprint arXiv*:2407.09930.

Astolfi, D. et al. (2021). Multivariate SCADA data analysis methods for real-world wind turbine power curve monitoring. *Energies*, 14.

Azevedo, H. D. M. et al. (2016). A review of wind turbine bearing condition monitoring: State of the art and challenges. *Renewable and Sustainable Energy Reviews*, 56, 368-379.

Cerezo, M. et al. (2022). Challenges and opportunities in quantum machine learning. *Nature Computational Science*, 2(9), 567-576.

Correa-Jullian, C. et al. (2022). Exploring Quantum Machine Learning and feature reduction techniques for wind turbine pitch fault detection. *Energies*, 15(8), 2792.

DOI: 10.59254/sbpo-2024-193539
https://proceedings.science/p/193539?lang=pt-br

Garg, S., and Ramakrishnan, G. (2020) Advances in quantum deep learning: An overview. *arXiv preprint arXiv:2005.04316*.

Havlíček, V. et al. (2019). Supervised learning with quantum-enhanced feature spaces. *Nature*, 567, 209-212.

Leite, G. D. N. P. et al. (2023). A robust fleet-based anomaly detection framework applied to wind turbine vibration data. *Engineering Applications of Artificial Intelligence*, 126.

Liu, Y., Arunachalam, S., and Temme, K. (2021) A rigorous and robust quantum speed-up in supervised machine learning. *Nature Physics*, 17, 1013-1017.

Mello, E. (2021). Data driven case study of a wind turbine main-bearing failure. In *Journal of physics*: Conference series, p. 012011. IOP Publishing.

Melnikov, A. et al. (2023). Quantum machine learning: from physics to software engineering. *Advances in Physics: X*, 8.

Munguba, C. F. L. et al. (2024). Ensemble learning framework for fleet-based anomaly detection using wind turbine drivetrain components vibration data. *Engineering Applications of Artificial Intelligence*, 133.

Pandit, R. K. et al. (2023). A Review of Predictive Techniques Used to Support Decision Making for Maintenance Operations of Wind Turbines. *Energies*, 16.

Papadopoulos, P., Coit, D. W., and Ezzat, A. A. (2021). Seizing opportunity: Maintenance optimization in offshore wind farms considering accessibility, production, and crew dispatch. *IEEE Transactions on Sustainable Energy*, 13, 111-121.

Schuld, M., and Petruccione, F. (2018). Supervised learning with quantum computers. *Springer*, Berlin.

Schuld, M. (2021). Supervised quantum machine learning models are kernel methods. *arXiv preprint arXiv:2101.11020*.

Smola, A. J., and Schölkopf, B. (2004). A tutorial on support vector regression. *Statistics and computing*, 14, 199-222.

Summerfield-Ryan, O., and Park, S. (2023). The power of wind: The global wind energy industry's successes and failures. *Ecological Economics*, 210.

Vieira, J. L. M. et al. (2024). Remaining Useful Life Estimation Framework for the Main Bearing of Wind Turbines Operating in Real Time. *Energies*, 17.

Wiese, B. et al. (2020). Estimating the remaining power generation of wind turbines—an exploratory study for main bearing failures. *Energies*, 13.

Yan, M. et al. (2020). Bearing remaining useful life prediction using support vector machine and hybrid degradation tracking model. *ISA transactions*, 98.

Zhou, X. et al. (2024). Quantum kernel estimation-based quantum support vector regression. *Quantum Information Processing*, 23(1), 29.

DOI: 10.59254/sbpo-2024-193539
https://proceedings.science/p/193539?lang=pt-br